Sensor Development to Utilize Underwater Electric Potential (UEP) Fields to Navigate the Underwater Areas of Ship Hulls

Caglar Erdogan
Florida Institute of Technology

Sensor Development to Utilize Underwater Electric Potential (UEP) Fields to Navigate the Underwater areas of Ship Hulls

The Link Foundation Ocean Engineering and Instrumentation

Fellowship Program Final Report

Prepared by Caglar Erdogan

Melbourne FL

September 2019

Contents

Executive Summary

Underwater electric potential fields occur due to natural reasons, such as changes in atmosphere, ionosphere, magnetosphere, and movements of water bodies in the ocean, or artificial reasons, such as stray and controlled electric currents, or both. Electric potential fields around ship hulls are mainly generated due to corrosion protection systems and dissimilar materials. The electric field intensity over an impressed current anode of a large cruise ship operating in with seawater with a resistance of 20 Ω-cm is around 90 mV/cm, whereas it is between 0.4 and 1 mV/cm on a propeller for the same ship. The theoretical field intensities obtained from an impressed current cathodic protection (ICCP) system example on COMSOL are 22.5 mV/cm and between 1.25 and 6.25 mV/cm on the surface of the anode and the propeller, respectively.

Elasmobranch fishes are able to sense fields as low as 5 nV/cm and the most sensitive commercially available instrument can detect fields strengths as low as 10 nV/cm at 1 Hz. Commercially available sensors utilize either Ag/AgCl or carbon fiber.

This research has investigated the use of Calomel reference electrodes to detect underwater electric fields. Experiments have been conducted to determine the sensitivity of Calomel reference electrodes. The first experiment, a simple replication of an ICCP system involving two electrodes and a power supply has been utilized in seawater at Florida Tech's Port Canaveral test site to generate electric potential fields. The potential gradient field was measured with two Calomel reference electrodes. The experiment showed that the movement of the water column increases the fluctuation of the voltage readings. Therefore, it was difficult to determine the sensitivity of Calomel reference electrodes. However, the data showed that the potential difference between two Calomel reference electrodes can be utilized for directionality. The second experiment was conducted in a water tank with both fresh water and seawater. The experimental design entails two stainless steel electrodes and two Calomel reference electrodes for potential measurements. A PVC pipe was utilized to obtain uniform electric potential field distribution to determine the sensitivity of Calomel reference electrodes. The result showed that the electric potential gradient for fresh water was higher than the seawater due to high resistivity of fresh water. The settling and response time of Calomel REs were still high in a stationary condition for sensitivity measurements with limited current output of the galvanostat.

Background

Electric potential fields are present in most underwater environments. In 1832, Faraday first realized that seawater flowing through earth's steady magnetic field generates eddy currents in the sea. This was the first time that induced electric fields by steady ocean currents were investigated. He also made predictions about the river Thames possessing induced electric fields due to the motion of the water [1]. However, he couldn't justify his predictions on the existence of these fields due to the absence of proper instrumentation. In 1873, Scottish mathematical physicist, James Clerk Maxwell synthesized all the experimental work on electricity and magnetism of Coulomb, Oersted, Ampere, Faraday, and others into four mathematical equations, called Maxwell's equations [2]. These equations are the fundamental equations of modern electromagnetism.

Electric potential fields may be grouped into two categories depending on the source, natural and artificial. The natural fields originate from both external and internal sources. External sources include changes in atmosphere, ionosphere, and magnetosphere, such as Schumann resonant fields and telluric fields. Internal sources, on the other hand, are due to the movement of water such as steady currents and periodic tides. Typical values for the gradient fields in the ocean are usually less than 0.5 μV/cm. Ocean gyres generate between 0.05 and 0.5 μV/cm and strong tidal currents 0.25 μV/cm [3]. Moreover, the maximum tidal signals measured for diurnal (O1) and lunar semidiurnal (M2) tides are 10 mV/km and 100 mV/km, respectively [4].

Natural fields are utilized by elasmobranch fishes, such as sharks, rays and skates to hunt and navigate underwater. These are sensed with an ampullary electrosensory systems called ampullae of Lorenzini. These primary electric field sensing canals are modified parts of the lateral line system [5]–[9]. They are gel filled and highly sensitive to DC and low-frequency AC electric fields [3]. Each electrosensory receptor is activated by electrical potential changes in the vicinity. The calcium ions flow in and potassium ions flow out in the cell which stimulates the nerve cells.

Sharks are able to sense field intensities as low as 5 nV/cm [8], [10], [11], and they use two methods, passive and active, to sense these fields. Passive sense involves sensing the potential gradients generated by their prey and ocean streams. Active sense requires sharks to swim through earth's magnetic field to generate electrical potential differences. The field strength depends on the swimming speed of the shark. Swimming speeds of 50 cm/s can result in 0.1 to 0.2 μV/cm voltage gradient generation [3].

Artificial sources for electric fields originate from stray and controlled electric currents, such as power grids, electric trains, corrosion currents from submerged metals in seawater, corrosion protection systems, and underwater powerlines for offshore renewable energy systems [4], [12], [13]. Artificial potential gradient fields are utilized to detect coating holidays, electric signatures of ships, location of the corroding metals, oil and gas reservoirs, and sea mines.

Potential gradient fields formed around ships and structures are generated by cathodic protection systems and dissimilar metals. These fields can be modeled as an electric dipole [14]–[16], and their intensities are functions of the conductivity of the medium, the current density and the distance between electrodes.

The present practice to measure the potential of metals and gradient fields in seawater is by the use of reference electrodes. Reference electrodes are made from stable half cell reactions which are not affected by the composition of the analyte, and ideally, they should have zero impedance [17], [18]. These are given a potential value reference to a standard hydrogen electrode (SHE). The most common reference electrodes for potentiometric measurements used in seawater are silver/silver chloride (Ag/AgCl) [19]. These comprise a silver surface overlain by silver chloride. This forms a stable half cell potential which is determined by the chloride ion concentration. There are five types of Ag/AgCl reference electrodes, including seawater, liquid-based, gel-based, solid melt, and all-solid-state electrodes. The main difference between these electrodes is the anion that surrounds the electrode. For seawater reference electrodes the electrode is immersed directly into the seawater environment. The liquid-based electrode contains an aqueous solution of known potassium chloride (KCl) molarity, gel-based electrodes have hydrogel trapped KCl solution, solid melt electrodes are built with the solid melt of the KCl, and all-solid-state has an all-solid reference element.

Ship Hull Navigation

Ship hulls present large surface areas which are difficult to navigate when present in complex environments with turbid waters containing a lot of floating particles. In these situations the reliability of the navigation sensors are diminished [20]. This, research investigated the use of the electric potential fields generated by ICCP systems as an aid to underwater navigation. This will require the application of sensors that are able to detect low level changes in potential and can be incorporated into the navigation systems of underwater vehicles.

ICCP system entails a DC power source (usually rectified AC), inert anodes as a current source, reference electrodes to measure the ship hull potential, and control systems to regulate the current. The basic working principle of the ICCP system is that the electrical potential readings from the zinc or silver/silver chloride reference electrodes are fed back to the control panel that then applies the required current output from the anode to maintain the potential [21]. In a completed corrosion control system, the current flows from the anode (positive electrode) through the seawater (electrolyte) to the cathode (negative electrode) which includes the ship hull, propeller, rudder, thrusters, stabilizers etc.). These are the areas that need to be protected. The current will generate potential gradient fields around the ship hull due to the ohmic drop.

It is impossible to predict with any precision the cathodic protection current demand of a ship due to the age and condition of the hull, the geometry, the cathodic protection design (impressed current and sacrificial), and the environmental conditions. For example, the potential field gradient generated at the surface of a 50 cm diameter impressed current anode on a large cruise ship operating at 9 amps, a current density of 45 amps/m^2 and seawater resistivity of 20 Ω-cm is 90 mV/cm, since it is a product of current density and seawater resistivity. However, this surface potential gradient will diminish as the current spreads over the surface of the hull. A large proportion of the current will be taken by the propeller and the rest will enter the hull over areas of where the coating has low resistance due to damage or poor application. The current demand for cathodically protected coated and uncoated steel under static conditions has been defined by Berendsen [22], which are 33 and 130 mA/m^2 respectively and he suggests that the design current demand for bronze propellers is about 500 mA/m^2. This would create an ohmic drop at the surface of a ship hull.

Table 1 Ohmic Drop

	Current Density (mA/m^2)	Seawater Resistivity (Ω.cm)	Ohmic Drop (mV/cm)
Hull	Coated: 33 Uncoated: 130	20	Coated: 0.066 Uncoated: 0.260
		25	Coated: 0.082 Uncoated: 0.325
Propeller	200 - 500	20	0.4 - 1
		25	0.5 - 1.25
Anode	45000	20	90
		25	112.5

Numerical Model by COMSOL Multiphysics®

A numerical model developed by COMSOL Multiphysics® was utilized to determine the underwater electric potential (UEP) gradient field generated by an ICCP system around a ship hull [23]. A 36 m long boat with two Nickel Aluminum Bronze (NAB) propellers and alloy 625 shafts, two anodes and two Ag/AgCl reference electrodes has been used for this example. The NAB propeller, the anode and the reference electrode are located at 1.5, 8, and 14 m away from the aft of the boat, respectively.

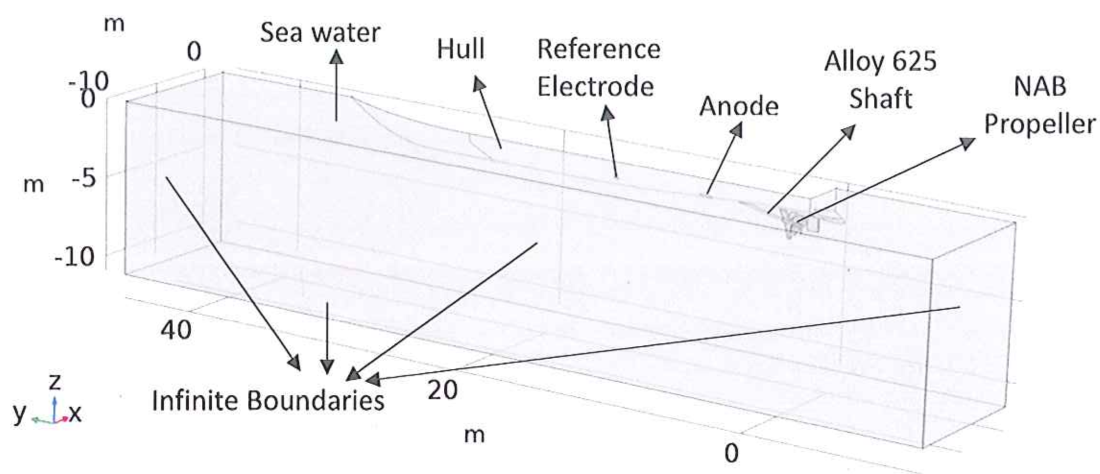

Figure 1 Model developed by COMSOL®

The UEP field for the half of the boat due to the exact symmetry has been analyzed using Butler-Volmer equation with the parameters shown below (Table 2). Butler-Volmer equation is

$$j = j_0 \cdot \left\{ exp\left[\frac{\alpha_a zF\eta}{RT}\right] - exp\left[-\frac{\alpha_c zF\eta}{RT}\right]\right\}$$

where:

j: electrode current density, A/m^2 (defined as j = Current/Area)

j_0: exchange current density, A/m^2

T: absolute temperature, K

z: number of electrons involved in the electrode reaction

F: Faraday constant

R: universal gas constant

α_a: so-called anodic charge transfer coefficient, dimensionless

α_c: so-called cathodic charge transfer coefficient, dimensionless

η: activation overpotential (defined as $\eta = E - E_{eq}$)

E: electrode potential, V

E_{eq}: equilibrium potential, V

Table 2 Parameters for Propeller and Shaft

E_{vsref}	-0.85 [V]	Ship hull potential vs reference, imposed by ICCP system
σ	4 [S/m]	Sea water conductivity
E_{eq_prop}	-0.31 [V]	Equilibrium potential of propeller vs. Ag/AgCl
i_{0_prop}	150 [mA/m^2]	Exchange current density of propeller
α_{a_prop}	0.78	Anodic transfer coefficient of propeller
α_{c_prop}	0.45	Cathodic transfer coefficient of propeller
E_{eq_shaft}	-0.18 [V]	Equilibrium potential of shaft vs. Ag/AgCl
i_{0_shaft}	1.3 [mA/m^2]	Exchange current density of shaft
α_{a_shaft}	0.44	Anodic transfer coefficient of shaft
α_{c_shaft}	0.57	Cathodic transfer coefficient of shaft
i_{lim}	5 [A/m^2]	Limiting current density at cathodes

In the example, the anode surface potential has been set to zero, since anode kinetics were unknown. The current density on the anode and propeller surface are 9 A/m^2 and between 0.5 and 2.5 A/m^2, respectively. The potential field gradient generated on the surface of the anode is 22.5 mV/cm, whereas it is between 1.25 and 6.25 mV/cm for the propeller surface.

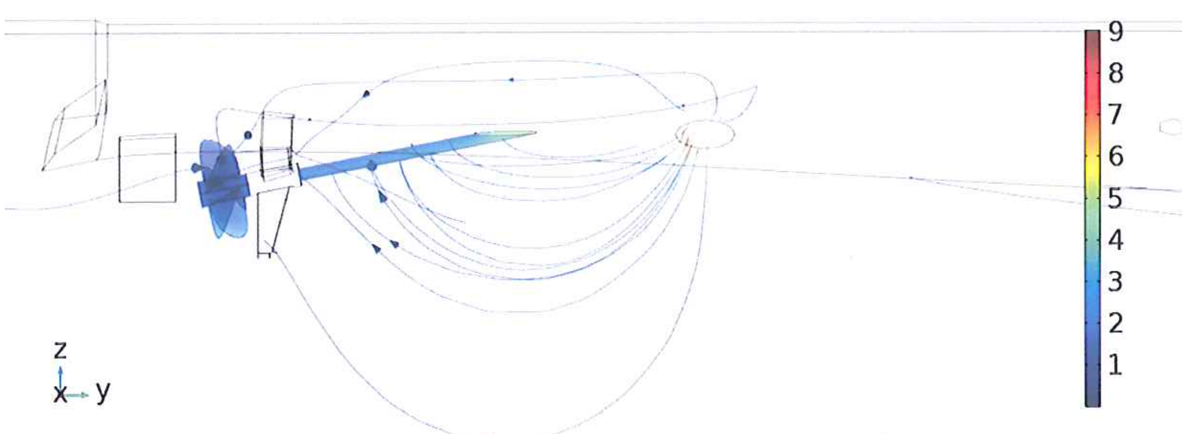

Figure 2 Current Densities (A/m^2) from COMSOL®

The sliced section of the electrolyte was investigated to determine the optimal range that the EUP gradient sensors may be used. It was positioned according to the location of the anode where the potential gradient is highest.

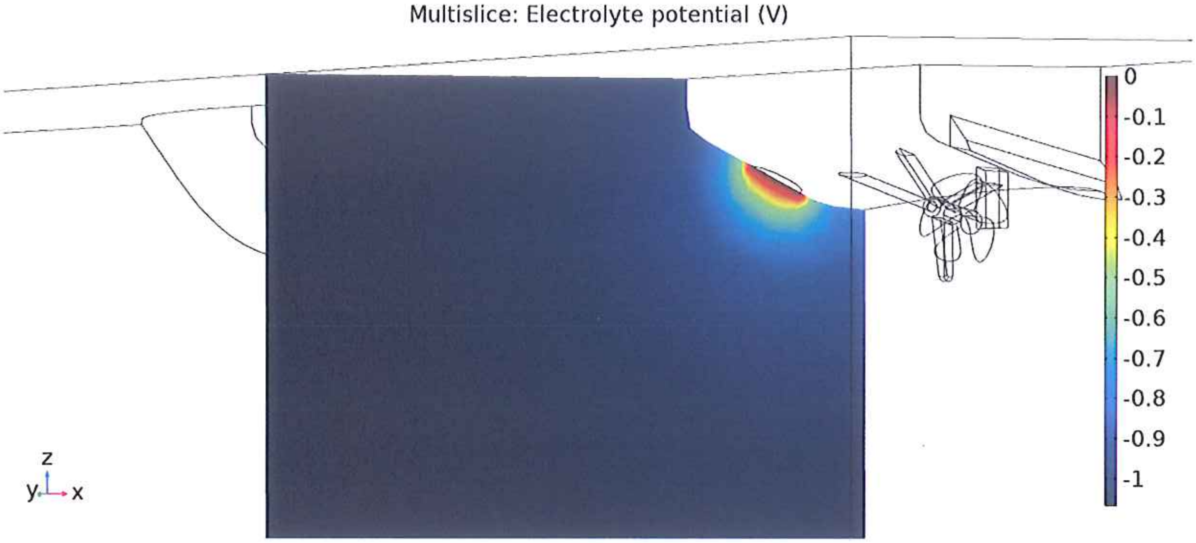

Figure 3 Electrolyte section investigated for the eletric potential change with distance from COMSOL®

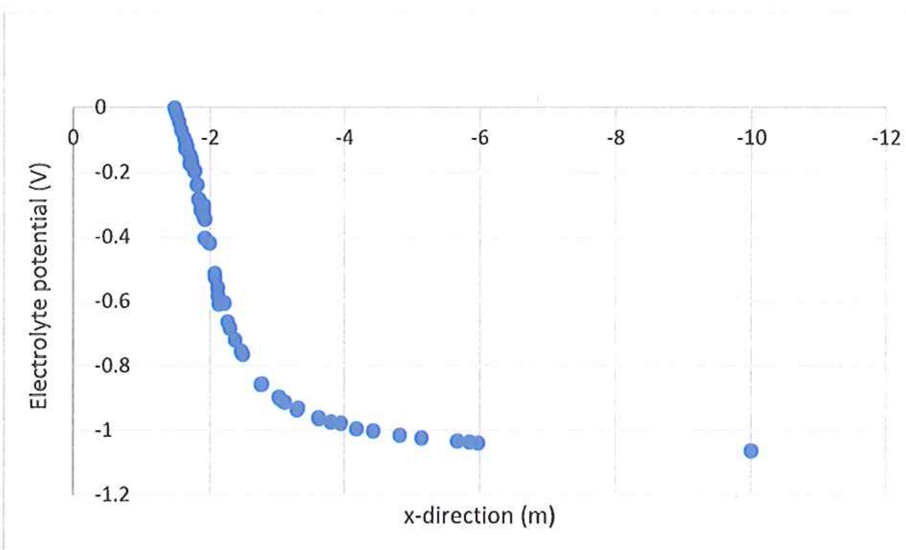

Figure 4 Electric potential change in x-direction from COMSOL®

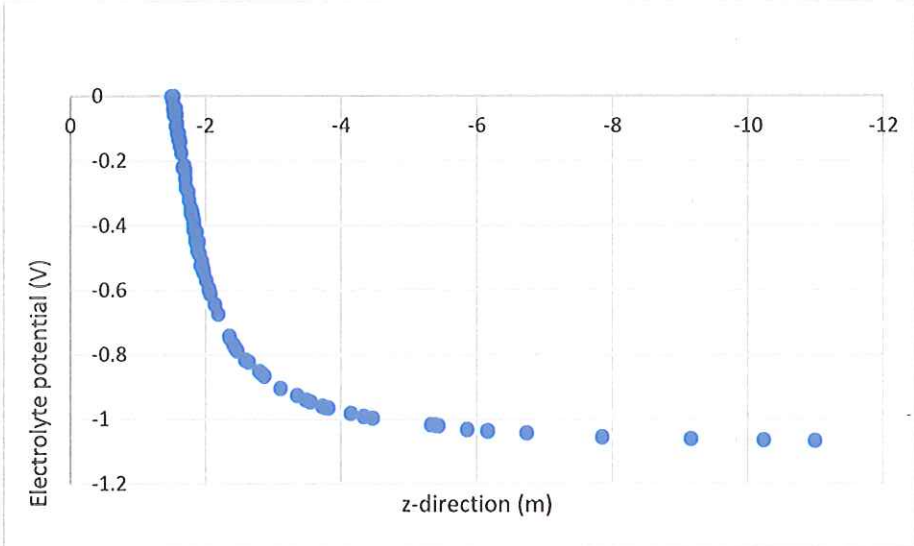

Figure 5 Electric potential change in z-direction from COMSOL®

The data in the x and z direction collected from the COMSOL showed that the potential gradient decreases with the distance (Figure 4 and Figure 5). The first couple of meters away from the anode may present the highest potential gradient values to be measured with a sensor.

Prior sensor studies

The ability of a sensor to detect low frequency electric fields in seawater is a fundamental requirement. Song, Zhang, and Zuo [24] have conducted an experiment to compare reference electrode materials, including Ag, zinc, graphite, carbon fiber, Saturated Calomel Electrode (SCE), all-solid-state Ag/AgCl, and conventional Ag/AgCl electrodes with respect to their DC resistance, AC impedance and voltage difference of the electrode pairs, which determines the sensitivity. They concluded that the all-solid-state Ag/AgCl electrode and carbon fiber electrode performed the best to measure the low and extra low-frequency electric fields. They found that the minimum voltage difference that could be detected by the all-solid-state Ag/AgCl electrode, commercial Ag/AgCl electrode, and carbon fiber electrode pairs were 20, 130, and 260 uV, respectively. However, the high impedance of Ag, SCE and conventional Ag/AgCl electrodes, and the unsteadiness of zinc electrodes were inadequate for low frequency measurements in seawater.

Ag/AgCl reference half cells have been utilized as potential difference sensors to determine the electric potential fields from corrosion protection systems [25]–[29]. Wimmer, Hogan, and Degiorgi [25] performed experiments to test their design of an Ag/AgCl sensor by using a simple dipole replicating the features of an ICCP system. The electric poles placed 250 cm apart at a depth of 82.398 cm below the water surface in a cylindrical tank covered with

0.76 mm thick neoprene. The resistivity of the water in the tank was 740 Ω-cm. The electric field sensor was placed 47.5 cm below the centerline of the dipoles and moved from one pole to the other. They minimize the variations between computational, analytical and measured electric fields by adjusting the sensor design. Wimmer and Degiorgi [26] indicated that the use of a sensor with differential potential sensing could detect the corrosion related electric potential fields.

Qualls et al. [28] and Ross et al. [29] have also developed a sensor with Ag/AgCl electrodes to detect UEP fields of moving vessels and these sensors were attached to an autonomous underwater vehicle (AUV) for field experiments [28], [29]. Both sensors were comprised of three orthogonal pairs of electrodes. The sensor developed by Qualls et al. [28] had a 3.81 cm diameter spherical polymer housing. The diameter and the length of the Ag/AgCl electrodes were 2 mm and 4 mm, respectively. The preamplifier was attached separately to the AUV. The electric fields were generated between two conductive plates attached to a 7.62 m long fiberglass boat at a known distance by AC electric currents at frequencies of 5, 10, and 20 Hz. The UEP field sensor at 10 m depth measured 41.5 mV/cm peak value of an electric field generated by a 10 Hz sinusoidal voltage when the boat was cruising. Whereas, the sensor by Ross et al. [29] had a 7.62 cm urethane elastomer compound spherical housing. The Ag/AgCl electrodes were 12 mm in diameter and 1 mm in length. The preamplifier was embedded in the center of the spherical housing. The noise floor of the reference electrode pairs was reported to be 100 μV/cm over the 0.02 Hz to 20 Hz bandwidth. 30 amps direct current (DC) current was impressed between two electrodes attached to the bow and the stern of the boat to create an electric field. When the boat was cruising, approximately 1 V/cm peak electric field magnitude was measured with the UEP field sensor at 10 m depth [28], [29].

Several commercially available electric field sensors have been developed with either Ag/AgCl or carbon fiber electrodes [30].

Table 3 Commercial Electric Field Sensors for Marine Use [30]

Manufacturer	Application	Model	Probe Type	Sensitivity (V/m)	Frequency Span (Hz)	Noise Floor (nV/√Hz @ 1 Hz)
Information Systems Laboratories Inc.	Harbor security, surveillance	MEFSS	Silver silver-chloride	6 nV/m @ 1 Hz	25	6
Ludwig Systemtechnik	Signature measurement	EMMS	Carbon fiber	Unk.	Unk.	Unk.
Polyamp AB	Signature measurement	UMISS	Carbon fiber	< 2 nV/m @ 1 Hz	0.003 – 1100	~ 1
Polyamp AB	Signature measurement	3-300/3-500	Carbon fiber	~ 2 to 3 nV/m @ 1 Hz	0.003 – 1100	~ 1
Subspection	Signature measurement	Ultra Sensitive	Silver silver-chloride	< 1 nV/m @ 1 Hz	0.001 – 5 0.5 - 1000	1
Subspection	Signature measurement	Portable	Silver silver-chloride	5 nV/m @ 5 Hz	0.005 – 5 1 – 1000	1
Subspection	Ranging, Signature measurement	Compact	Silver silver-chloride	< 2.5 nV/m @ 1 Hz	0.005 – 5 1 – 1000	2.5
Subspection	Harbor security	Miniature	Silver silver-chloride	~ 0.1 nV/m @ 1 Hz	0.001 – 1000	2.5
Ultra-PMES	Signature measurement	Compact 3-Axis	Silver silver-chloride	< 2.5 nV/m @ 1 Hz	DC to 3000	< 0.5

Measuring IR Drop Using Calomel Reference Electrodes

Preliminary experiments have been completed to evaluate the sensitivity and precision of calomel reference electrodes (REs) to measure IR drop.

Initial Experiment at Port Canaveral Site

Methods

The first set of experiments were conducted at Florida Tech's Port Canaveral test site. Two MMO cylindrical electrodes with 26 cm in length and 4.6 cm in diameter were utilized as an anode and cathode to generate the potential field. They were placed 100 cm apart in the water and connected to a PGS151 Potentiostat/Galvanostat. Electric currents from 0 to 300 mA with 50 mA increments were applied. Two OHAUS Saturated Calomel REs were positioned 20 cm apart from each other and placed to the center of the MMO electrodes. One of the two Calomel REs was marked with letter "A". The potential difference between REs was collected when RE "A" was pointing the east and the other one was west. The data collection was repeated after the REs were rotated 180 degrees. Electric potentials of MMO electrodes and differential potential of SCE REs were measured with multimeters.

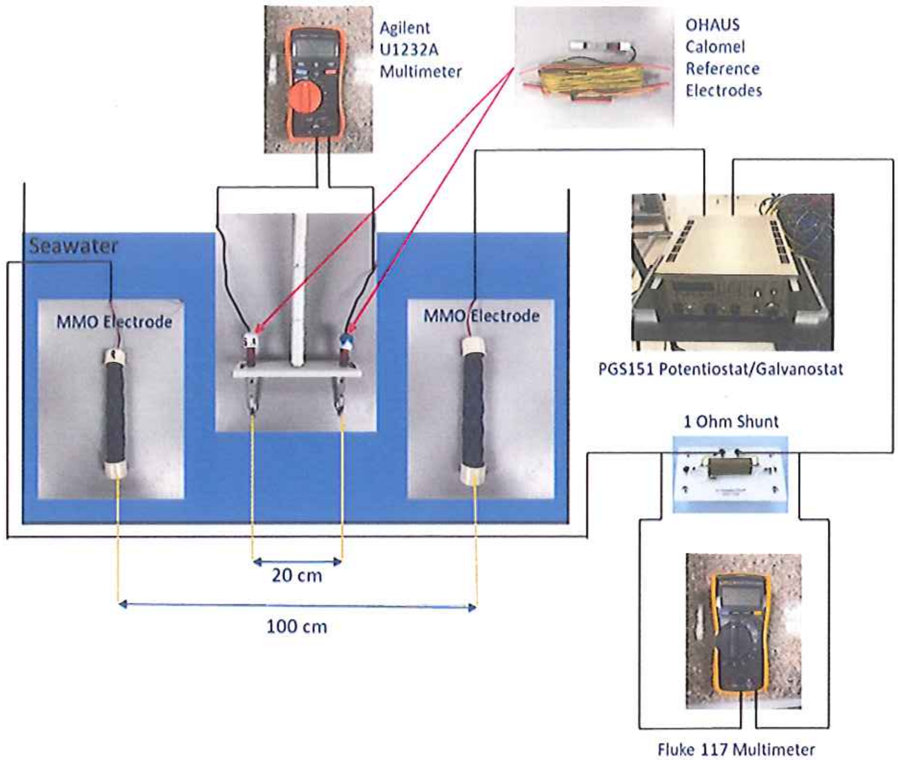

Figure 6 Experimental setup at Port Canaveral

Results

The UEP gradient is the measured potential difference divided by the distance. Both the collected and the calculated data was presented in Table 4.

Table 4 Measure potential and Potential gradient data

Current (mA)	Measured Potential (mV)		Gradient (mV/cm)
	A pointing east	A pointing west	
53	-1.9	-	-0.095
100	-3.7	-	-0.185
150	-5.6	-	-0.280
200	-7.5	-	-0.375
250	-9.3	-	-0.465
302	-11.2	-	-0.560
302	-	11	0.550
248	-	9.1	0.455
200	-	5.8	0.290
150	-	4.2	0.210
100	-	2.4	0.120
50	-	-0.4	-0.020

The potential gradient for both cases was plotted against the current to determine the sensitivity of the Calomel REs (Figure 7).

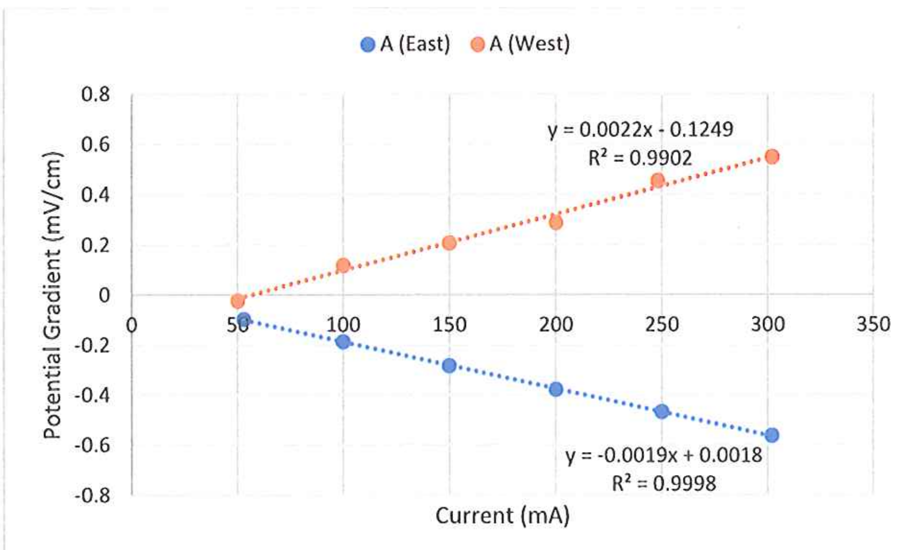

Figure 7 Potential gradient change with varied current

Discussion

The data was analyzed with the assumption of uniform distribution. The result shows that between the measured potential difference with Calomel REs for varying currents follows a linear trend (Figure 7). The positioning of the REs determines whether the potential gradient is increasing or decreasing. Therefore, the potential gradient difference from two

REEs can be used to determine the location of the anode (source) and the cathode (sink). It can provide directionality for underwater navigation. This experiment showed that one of the drawbacks of utilizing Calomel REs was that the time that they reach to equilibrium was affected by the environmental conditions, such as temperature and water flow speed.

Calomel REs Sensitivity Experiment in a Water Tank

Methods

The second set of experiments were conducted in a 570-liter water tank. Two 0.95 cm diameter stainless steel (SS) electrodes were placed 20 cm apart in a Polyvinyl chloride (PVC) pipe with a diameter of 2.54 cm and a length of 40 cm. Two OHAUS Saturated Calomel REs were placed 10 cm apart between the SS electrodes in PVC pipe. PVC pipe was used to channel the current flow through a known cross-sectional area and eliminate the dipole effect on the potential field distribution. A PGS151 Potentiostat/Galvanostat was connected to the SS electrodes and constant current applied. Multimeters were used to measure the potentials between the SS and Calomel REs separately. A one Ohm shunt was connected to the system to verify the actual output from the power source. (Figure 8).

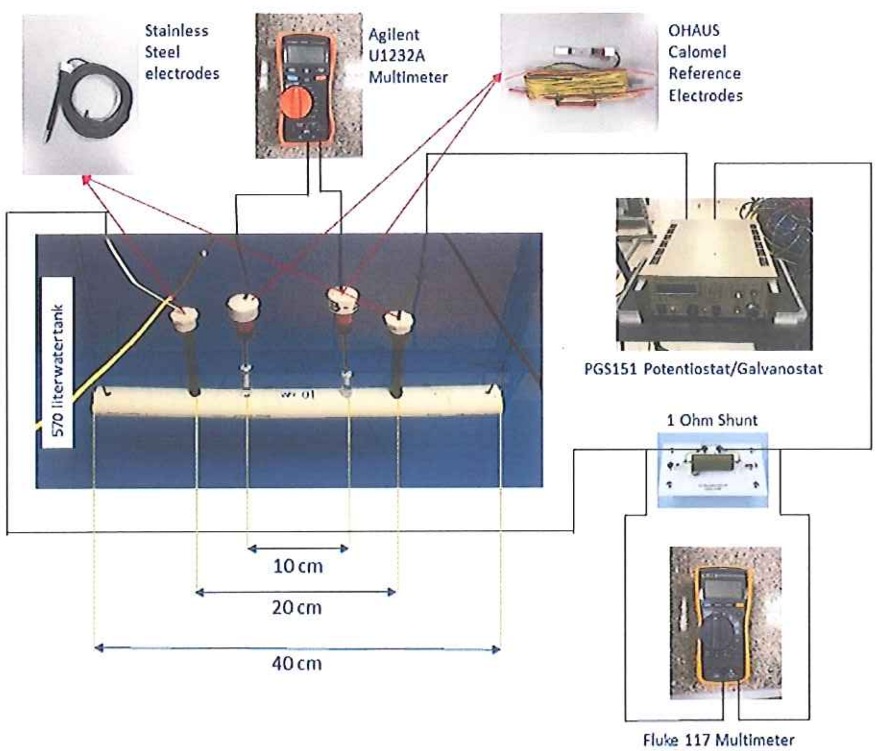

Figure 8 Experimental setup at the lab

The experiment was performed both in fresh water and seawater with the assumptions of uniform electric field distribution and no spreading. The conductivity was 0.45 mS/cm (0.2 ppt, 24.5°C) for fresh water and 43.89 mS/cm (28 ppt, 24.6°C) for seawater. SS and reference electrodes were submerged in the water tank. Constant current ranging from 1 μA to 50 μA was applied between the two electrodes by the PGS151 Potentiostat/Galvanostat. The potential difference between the Calomel REs and the potential of each electrode was measured using the Agilent multimeter for different current input values. The voltage drop measured with the Fluke multimeter over the shunt was used to verify the value displayed on the galvanostat was correct. The IR drop was calculated by dividing the potential gradient by the distance between REs.

Results

The equation utilized to calculate the resistance is,

$$R = \rho \times \frac{L}{A} \tag{1}$$

where R is the resistance (Ω), ρ is the resistivity (Ω-cm), L is the length (cm) between the electrodes, and A is the cross-sectional area (cm^2). Resistance can be calculated as the ratio of the voltage to the current according to Ohm's Law.

$$R = \frac{V}{I} \tag{2}$$

where R is resistance (Ω), V is voltage (Volts) and I is the current (Amps). When equation (1) is plugged into equation (2), the resistivity equation is

$$\rho = \frac{V}{L} \Big/ \frac{I}{A} \tag{3}$$

The equation to calculate IR drop then becomes;

$$IR\ Drop = Current\ Density\ \times Resistivity \tag{4}$$

where the units for current density and resistivity are A/cm^2 and Ω-cm, respectively. The measured and calculated IR drop values for fresh water and saltwater are presented in Table 5. Then the electric field intensities of fresh water and seawater were plotted (Figure 9).

Table 5 Data for IR Drop

	Fresh water		Seawater	
Applied Current (uA)	Measured IR Drop (mV/cm)	Calculated IR Drop (mV/cm)	Measured IR Drop (mV/cm)	Calculated IR Drop (mV/cm)
50	9.87	22.17	0.17	0.22
40	7.94	17.74	0.13	0.18
30	5.95	13.30	0.1	0.13
20	4.03	8.87	0.07	0.09
10	2.05	4.43	0.05	0.04
9	1.84	3.99	0.04	0.04
8	1.63	3.55	0.03	0.04
7	1.42	3.10	0.03	0.03
6	1.22	2.66	0.03	0.03
5	1.04	2.22	0.02	0.02
4	0.83	1.77	0.02	0.02
3	0.63	1.33	0.01	0.01
2	0.44	0.89	0.01	0.01
1	0.4	0.44	0.005	0.004

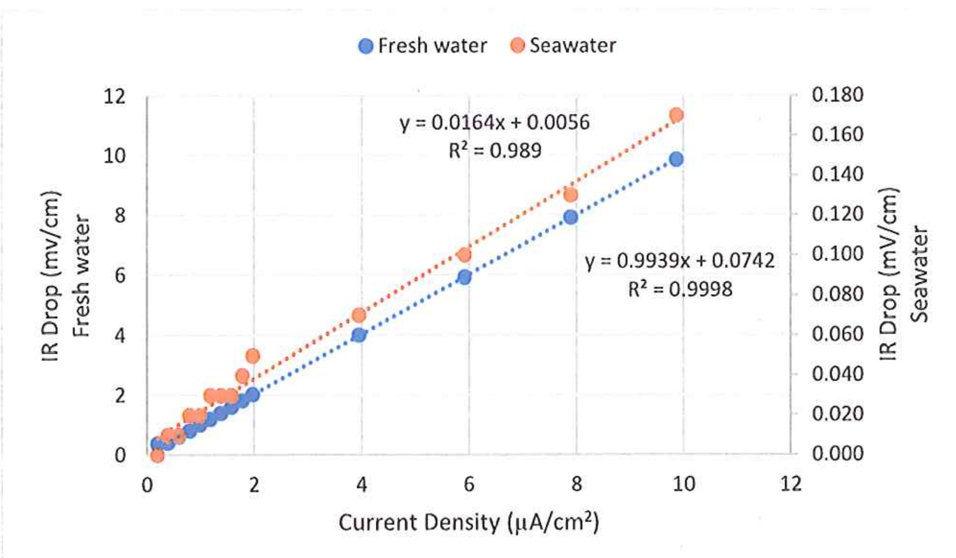

Figure 9 Measured Fresh water vs Seawater IR Drop

Discussion

Saturated calomel electrodes spaced at known distances can be used to measure IR drop in an electrolyte. A conductivity gauge was utilized to determine the conductivity of fresh water and seawater, which were 0.45 mS/cm and 43.89 mS/cm, respectively. Since the resistivity is the reciprocal conductivity, the resistivity of fresh water and seawater was 2222 Ω-cm and 22.78 Ω-cm, respectively. When constant current from 1 μA to 50 μA was applied through the electrolyte, the measured IR drop in fresh water was between 0.4 to 9.87 mV/cm, whereas it was between 0.005 to 0.17 mV/cm in seawater. This showed that the IR drop in fresh water is greater than seawater. The measured and calculated IR drop for fresh water showed higher differences than seawater due to the low conductivity of fresh water. However, the current densities generated by an ICCP system on a ship will probably be less than those used in these preliminary experiments.

Summary and Future Directions

Electric potential fields are generated due to natural and artificial sources in the marine environment. The magnitude of electric potential fields generated by natural sources are between 0.05 μV/cm and 0.5 μV/cm. The artificial source, such as a ship ICCP system may generate fields gradients 90 mV/cm and between 0.1 and 4 mV/cm on anode and propeller surface, respectively. Although to date the highest sensitivity of a commercially available sensor developed by Subspection is 10 nV/cm at 1 Hz, sharks have demonstrated their ability to sense potential gradient fields as low as 5 nV/cm.

The highly sensitive electrosensory organs of sharks are still not well understood. Scientists have studied the properties of the gel within the ampullae of Lorenzini to determine whether they contribute to the sensitivity of these organs. Zhang et al. [9] reported that the proton conductivity of the glycoprotein gel has been measured to be higher than any other biological material. However, the characteristics of this gel in the canals are still unknown [9], [31].

Highly sensitive underwater navigational aid sensor development requires utilizing new methods, since conventional Ag/AgCl reference electrodes with the liquid filling solution are susceptible to temperature, pressure and pH changes, and mechanical forces [19]. Therefore, microfabricated all-solid-state reference electrodes may be used for sensor development. Microfabrication reduces the cost, increases the analysis time, reliability, and repeatability [32]. All-solid-state reference electrodes can be easily miniaturized and integrated with other sensors for various applications. They can provide high stability for a longer time with less drift. One of the benefits of all-solid-state reference electrodes is that they may be utilized in junction with electroactive polymers or ionic liquids, which may contribute to the stability with high response time to measure the electric potential fields.

However, measuring and imaging the electric potential fields may be difficult even with a highly sensitive sensor since all type of materials including dielectric, conductive, semi-conductive, insulating, and triboelectric materials will distort the existing field [33]. Also, material locations and the size of the metallic components, as well as salinity, temperature, pH, and seawater flow speed around the hull may cause variations in the underwater electric fields [34].

Acknowledgement

Link Foundation – Link Ocean Engineering and Instrumentation Ph.D. Fellowship Program

References

[1] S. Maus, "Ocean, Electromagnetic Effects," in *Encyclopedia of Geomagnetism and Paleomagnetism*, D. Gubbins and E. Herrero-Bervera, Eds. Dordrecht: Springer Netherlands, 2007, pp. 740–742.

[2] F. T. Ulaby, *Electromagnetics for engineers*. Upper Saddle River, NJ: Pearson/Prentice Hall, 2005.

[3] L. A. Wilkens and M. H. Hofmann, "Behavior of Animlas with Passive, Low-Frequency Electrosensory Systems," in *Electroreception*, T. H. Bullock, C. D. Hopkins, A. N. Popper, and R. R. Fay, Eds. New York: Springer New York, 2005, pp. 229–263.

[4] A. Kuvshinov, A. Junge, and H. Utada, "3-D modelling the electric field due to ocean tidal flow and comparison with observations," *Geophys. Res. Lett.*, 2006.

[5] G. De Iuliis and D. Pulera, "The Shark," in *The Dissection of Vertebrates: A Laboratory Manual*, 3rd ed., Elsevier/Academic Press, 2007, pp. 63–69.

[6] A. J. Kalmijn, "Detection and processing of electromagnetic and near-field acoustic signals in elasmobranch fishes," *Philos. Trans. R. Soc. B Biol. Sci.*, vol. 355, no. 1401, pp. 1135–1141, 2000.

[7] R. K. Adair, R. D. Astumian, and J. C. Weaver, "Detection of weak electric fields by sharks, rays, and skates," *Chaos*, vol. 8, no. 3, pp. 576–587, 1998.

[8] M. G. Paulin, "Electroreception and the compass sense of sharks," *J. Theor. Biol.*, vol. 174, no. 3, pp. 325–339, 1995.

[9] X. Zhang *et al.*, "Structural and Functional Components of the Skate Sensory Organ Ampullae of Lorenzini," *ACS Chem. Biol.*, vol. 13, no. 6, pp. 1677–1685, 2018.

[10] G. W. Swain, E. R. Mueller, and D. R. Polly, "The Design and Installation of a Cathodic Protection System for the Living Seas, Epcot Center," *Mater. Perform.*, vol. 33, no. 10, p. 21, 1994.

[11] T. C. Tricas and B. A. Carlson, "Electroreceptors and magnetoreceptors," in *Cell Physiology Source Book*, Fourth Edi., Elsevier Inc., 2012, pp. 705–725.

[12] P. Tishchenko, "Electric Field of the Ocean Induced by Diffusion," *J. Electromagn. Anal. Appl.*, vol. 07, no. 01, pp. 10–18, 2015.

[13] R. H. Tyler, F. Vivier, and S. Li, "Three-dimensional modelling of ocean electrodynamics using gauged potentials," *Geophys. J. Int.*, vol. 158, no. 3, pp. 874–887, Jul. 2004.

[14] R. Adey and J. M. W. Baynham, "Predicting corrosion related signatures," *WIT Trans. Eng. Sci.*, vol. 54, pp. 213–223, 2007.

[15] I. Jeffrey, "Electromagnetic signature modeling and reduction," *Naval Architect*, no. AUG. SUPPL. pp. 22–23, 1999.

[16] Y. S. Kim, S. K. Lee, H. J. Chung, and J. G. Kim, "Influence of a simulated deep sea condition on the cathodic protection and electric field of an underwater vehicle," *Ocean Eng.*, vol. 148, no. December 2016, pp. 223–233, 2018.

[17] Metrohm, "Reference Electrodes and Their Uses," *Autolab Application Note EC02*, 2011. [Online]. Available: https://www.metrohm-autolab.com/download/Applicationnotes/Autolab_Application_Note_EC02.pdf.

[18] T. G. Nevell and F. C. Walsh, "Reference electrodes," *Trans. IMF*, vol. 70, no. 3, pp. 144–147, Jan. 1992.

[19] U. Guth, F. Gerlach, M. Decker, W. Oelßner, and W. Vonau, "Solid-state reference electrodes for potentiometric sensors," *J. Solid State Electrochem.*, vol. 13, no. 1, pp. 27–39, Jan. 2009.

[20] N. Servagent *et al.*, "Electrolocation sensors in conducting water bio-inspired by electric fish," *IEEE Sens. J.*, vol. 13, no. 5, pp. 1865–1882, 2013.

[21] Cathelco, "ICCP Hull Corrosion Protection Systems The Problem of Corrosion," 2017. [Online]. Available: http://www.shipserv.com/ShipServ/pages/attachments/59925/Cathelco C-Shield ICCP Brochure.pdf.

[22] A. M. Berendsen, "Cathodic Protection," in *Marine Painting Manual*, Dordrecht: Springer Netherlands, 1989, pp. 240–264.

[23] COMSOL Multiphysics® v. 5.4, "Corrosion Protection of a Ship Hull," 2019. [Online]. Available: https://www.comsol.com/model/ship-hull-iccp-14565.

[24] Y. S. Song, K. Zhang, and P. Zuo, "Choice of Electrode Material for Detecting Low Frequency Electric Field in Sea Water," *Adv. Mater. Res.*, vol. 239–242, pp. 137–140, May 2011.

[25] S. A. Wimmer, E. A. Hogan, and V. G. DeGiorgi, "Dipole modelling and sensor design," in *Simulation of Electrochemical Processes II*, 2007, vol. I, no. April 2007, pp. 143–152.

[26] S. A. Wimmer and V. G. Degiorgi, "Detecting Damage Using Electric Field Measurements : A Computational Sensitivity Study," Washington, DC, 2014.

[27] L. Demilier *et al.*, "Corrosion related electromagnetic signatures measurements and modelling on a 1:40 th scaled model," in *Simulation of Electrochemical Processes II*, 2007, vol. I, pp. 235–244.

[28] S. R. Qualls *et al.*, "Underwater electric potential measurements using AUVs," in *OCEANS 2015 - MTS/IEEE Washington*, 2015, pp. 1–4.

[29] R. Ross *et al.*, "Underwater electric field measurement and analysis," *Proc. MTS/IEEE Ocean. Conf. Exhib. (OCEANS 2017)*, 2017.

[30] M. Slater and A. Schultz, "Electromagnetic field study: Summary of commercial

electromagnetic field sensors for the marine environment," 2010.

[31] B. R. Brown, J. C. Hutchison, M. E. Hughes, D. R. Kellogg, and R. W. Murray, "Electrical characterization of gel collected from shark electrosensors," *Phys. Rev. E*, vol. 65, no. 6, p. 061903, Jun. 2002.

[32] M. W. Shinwari, D. Zhitomirsky, I. A. Deen, P. R. Selvaganapathy, M. J. Deen, and D. Landheer, "Microfabricated Reference Electrodes and their Biosensing Applications," *Sensors*, vol. 10, no. 3, pp. 1679–1715, Mar. 2010.

[33] E. R. Generazio, "Electric potential and electric field imaging," in *AIP Conference Proceedings*, 2017.

[34] M. Hirota, "A method to measure ship's underwater electric field from deck," in *Proceedings of the 2000 International Symposium on Underwater Technology (Cat. No.00EX418)*, 2000, pp. 224–228.

Appendix

The Initial Proposal

The Application of a Modulated Impressed Current Cathodic Protection (ICCP) System to Aid Underwater Navigation on Steel Structures Using Passive Electric Sense

Caglar Erdogan. Link Foundation Application. February 2018

The hypothesis developed for my PhD dissertation is that the current generated by an impressed current cathodic protection (ICCP) system may be modulated to create a potential field which can then be used by sensors to navigate the underwater areas of ship hulls and other underwater steel structures. The navigation systems most commonly used in underwater robots are vision-based, sonar guidance, a mix of sonar and vison, or magnetic field sensing. In complex environments with turbid waters, the reliability of the sonar signals and visual sensors are reduced. Electrolocation sensors, inspired by the electric field sensing organs of marine animals utilized for target localization and communication, will be used to address this problem. There are two forms of electrolocation, passive and active. Sharks, sturgeons and catfish utilize passive electrolocation to sense the weak bioelectric fields emitted by the prey and to navigate by using existing telluric electric fields. On the other hand, active localization working principles involve both emitting and sensing the electric field like in other active sensing systems such as radar and sonar.

This research will investigate a new method for active electrolocation on steel structures by modulating the ICCP current output to create potential fields that may be used as a mean of underwater navigation. Cathodic protection systems and underwater coatings are designed to protect the integrity of marine structures by preventing corrosion. The ICCP system includes a DC power source, inert anodes, reference electrodes, and a control system to provide the current. The basic working principle is that the electrical potential readings from the zinc or silver/silver chloride reference electrodes are fed back to the control panel that then determines the current output from the anode to prevent corrosion. The current flows from the anode (positive electrode) through the seawater to the cathode (negative electrode) which is the area that needs to be protected. The current flowing through the water creates potential fields due to IR drop. This can be detected with electric sensors designed to measure potential gradient.

Most of the prior research in this field has been based on the biomimicry of shark and ray electro sensing. A successful electric sensor for active electrolocation has been designed and implemented under the European project ANGELS. The system involves multiple metallic electrodes one of which acts as a current emitter and the others to receive the current. Data from this and other research will be used to develop finite element models that will used to design the sensors and control systems.

Field testing of the method will be conducted at the FIT test site located at Port Canaveral. The facility includes an 8x30' 1/4inch thick steel plate coated with ship hull coatings and a

SeaBotix ROV on which to mount the sensors. An ICCP system with signal modulating capabilities will be installed on the steel plate and the system evaluated for underwater navigation.